Shape-and-solder-directed self-assembly to package semiconductor device segments

Wei Zheng and Heiko O. Jacobs[a]

Department of Electrical and Computer Engineering, University of Minnesota, 200 Union Street SE, Minneapolis, Minnesota 55455

The self-assembly and packaging of integrated semiconductor device segments have been accomplished by combining geometrical shape recognition with site specific wetting and binding involving liquid solder. Components with complementary shapes were fabricated to recognize and encapsulate functional semiconductor devices. The components were suspended in water and agitated using a pulsating liquid flow. Two hundred AlGaN/GaN light-emitting diodes with a chip size of 380×330 micrometers were assembled and packaged with a yield of 95% in 2 min. The self-assembly procedure forms electrical interconnects between three-dimensional shaped objects and provides a route to parallel assembly of hybrid microsystems. © *2004 American Institute of Physics*. [DOI: 10.1063/1.1807017]

Fabrication strategies that rely on mechanisms of self-assembly are widely recognized as inevitable tools in nanotechnology. Self-assembly is not limited to the nanometer length scale. Methods of directed self-assembly have the potential to overcome the limitations of robotic assembly and enable multicomponent microsystems manufacturing in three dimensions.[1–10] Previous demonstrations of directed self-assembly to generate functional electrical microsystems include the coplanar integration of segmented integrated circuit devices into two-dimensional "superchips" using capillary forces,[1,2] shape-directed fluidic methods that position electronic devices on planar surfaces using shape recognition and gravitational forces,[3,4] liquid solder-based self-assemblies that use the surface tension between pairs of molten solder drops to assemble a three-dimensional electrical network, ring oscillators, and shift registers,[5,6] capillary force-directed self-assembly that uses hydrophobic–hydrophilic surfaces patterns and photocurable polymers to integrate micro-optical components, micromirrors, and semiconductor chips on silicon substrates,[7–9] and solder-receptor-directed self-assembly where metal contacts on segmented semiconductor devices bind to liquid solder-based receptors to assemble and electrically connect devices on planar and nonplanar surfaces.[10]

Here, we demonstrate directed self-assembly of semiconductor devices by combining three-dimensional shape recognition with surface-tension-driven self-assembly involving liquid solder. Our procedure uses geometrical shape recognition to identify different components and subsequent specific binding to form mechanical and electrical interconnects. Compared with existing self-assembly techniques, it provides a high distinguishing power between different components, mechanical strength, and electrical functionality of the assembled system; we call this method shape-and-solder-directed self-assembly. We apply this concept of shape recognition and subsequent binding between different components to package semiconductor devices. We demonstrate the self-assembly and packaging of two hundred AlGaN/GaN

light-emitting diodes (LEDs) in 2 min, with a yield of 95%.

The experimental strategy for the self-packaging of semiconductor device segments is illustrated in Fig. 1(a). To construct a system where the function can be tested visually, we used LEDs as device segments—unpackaged AlGaN/GaN LEDs with a chip size 380×330 μm wide, and 80 μm tall (Lginnotek, Korea). To host, protect, and electrically connect the LEDs, we fabricated encapsulation units out of 500 μm thick Pyrex wafers (Corning 7740, Universitywafer, Boston, Massachusetts). To recognize the LEDs during the encapsulation process and to distinguish between encapsulation units themselves, we formed a complementary shaped 100 μm deep truncated pyramidal opening in the center of the encapsulation units. The bottom face of the opening was 400×350 μm wide. Each opening exposed two
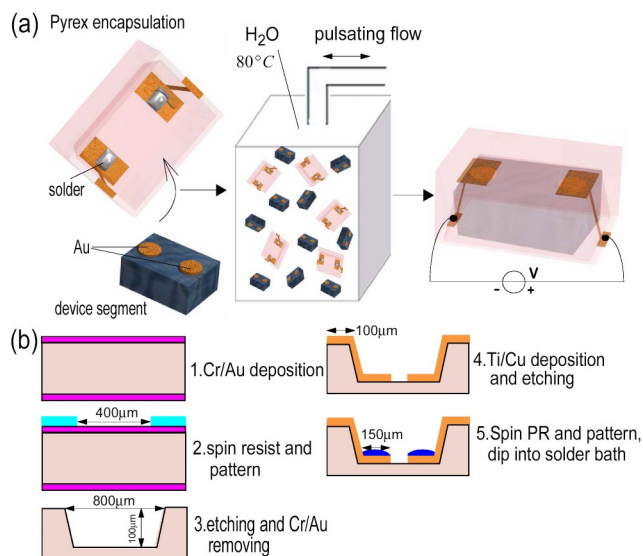

FIG. 1. (Color online) The strategy to assemble and package semiconductor chips by shape-and-solder-directed self-assembly. (a) Chip encapsulation in water at a temperature of $80\,^\circ$C where the solder is liquid. Agitation is provided using a pulsating liquid flow. The components self-assemble and form a circuit path between device layers that allow testing in a surface mount device configuration. (b) Fabrication procedures of Pyrex encapsulation units by surface micromachining and etching.

[a]Author to whom correspondence should be addressed; electronic mail: hjacobs@ece.umn.edu

3635   © 2004 American Institute of Physics

solder coated areas, 150×150 μm in size, to wet and bind to correspondingly shaped gold-coated areas on the LED. During the self-assembly, the surface of the liquid solder wets and binds to the two gold-coated contacts on the front side of the LED segment, and the minimization of the free surface area of the liquid solder drives the assembly into a stable aligned position. The solder also provides the electrical connection required to operate the device and the mechanical bond required to hold the assembly together. We used a low-melting alloy (Y-LMA-117, mp$\sim 47 °$C, Small Parts, Miami Lakes, Florida) of bismuth, lead, tin, cadmium, and indium as solder. This solder has been used in previous self-assembly experiments[10,11] because it has a high surface energy (~ 400 mJ/m^2) and a sufficiently low-melting point to allow the assembly to be carried out in water.

The assembly was carried out inside a rectangular glass container (12 mm on each side and 45 mm high) filled with 4.5 mL of deionized (DI) water at a temperature of $80 °$C. The solution was made slightly acidic (pH~ 2.5) with sulfuric acid to remove metal oxide from the surface of the solder drop; an oxide layer—if sufficiently thick—blocked the wetting of the metal surface. A pulsating liquid flow was used to agitate the components. The pulsating flow was delivered using a 30 mm Pasteur pipette by automatic compression of a 1.3 mL bulb using a crankshaft that is driven by a motor. The frequency of pulsating liquid can be adjusted between 0 and 4 Hz by changing the motor's rotation speed.

All of the components were fabricated by standard micromachining [Fig. 1(b)]. In brief, the Pyrex wafer was coated with 25 nm Cr and 250 nm Au using an electron-beam (e-beam) evaporator. The substrate was spincoated with photoresist (Microposit 1813, Shipley, Phoenix, Arizona), exposed, developed, and etched in 4 KI: 1 I$_2$: 40 H$_2$O for Au and 1 HCl: 1 Glycerine: 3 H$_2$O for Cr. The tapered opening was formed by etching in 20 HF (49%): 14 NHO$_3$ (69%): 66 H$_2$O for 2 h. After removing the metal layer, the glass wafer was coated with 25 nm Ti and 800 nm copper using an e-beam evaporator. Shipley Eagle 2100 photoresist was electroplated on the wafer using a dc voltage (50 V) for 30 s at $35 °$C. After a softbake at $80 °$C for 2 min, the photoresist was exposed and developed. The exposed copper was etched in an aqueous ferric chloride solution (1.4 g of FeCl$_3$ per ml of H$_2$O, pH 1.3) and the Ti was etched in 10:1 buffered oxide etchant. After removing the Eagle 2100 photoresist, Shipley 1805 photoresist was spun on the substrate and patterned to expose selected copper areas for solder wetting. The exposed copper was coated with a low-melting point solder by immersing the substrate into a solder bath. Finally, the wafer was diced to obtain the Pyrex encapsulation units.

Figure 2 illustrates the experimental realization of the chip-encapsulation procedure with 1000 LED chips and 200 encapsulation units in the assembly solution. The self-assembly process [Figs. 2(a)–2(d)] reached a steady state in 2 min. The assembly process was non-linear. To record the progression of the self-assembly [Fig. 2(e)], we interrupted the assembly process and counted the number of components that had assembled after 20 s time increments. The progression was faster in the beginning and slowed down as the assembly process reached the asymptotical limit. The observed slowdown can be explained by the reduction of available encapsulation units as the assembly proceeds. We also noticed that the number of available LEDs influenced the
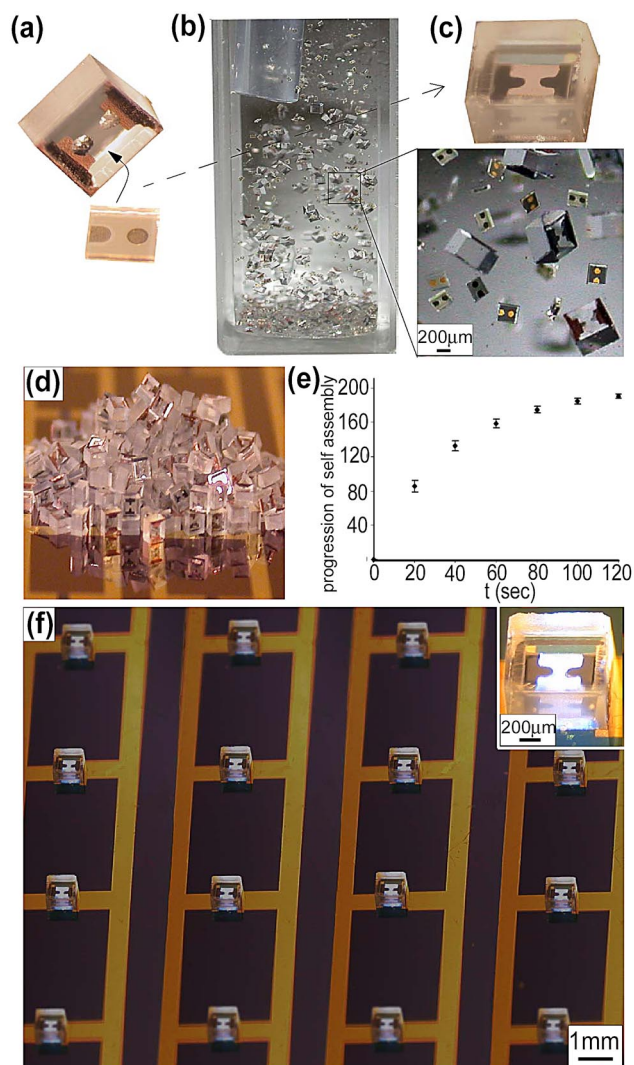

FIG. 2. (Color online) Experimental realization and testing of LED chips that were assembled and packaged by shape-and-solder-directed self-assembly. (a) Photographs of device components before chip encapsulation. (b) Images of the agitated components during the chip encapsulation process. (c) Photograph of a single device after chip encapsulation. (d) Photograph of an ensemble of 200 encapsulated devices that have been assembled in 2 min. (e) The progression of the self-assembly as a function of assembly time. Error bars show the standard deviations of three independent experimental data sets after every 20 s time increments. (f) Testing of an array of self-assembled LEDs that are mounted by hand on a printed circuit board. Inset shows a closeup.

overall duration of the self-assembly process. For example, with 500 LEDs and 200 encapsulation units in the assembly solution, the assembly process took 6 min to reach steady state, whereas with an increased number of 1000 LEDs it took only 2 min. Our hypothesis is that the number of excess LEDs defines the capture probability at a certain level of agitation. Increasing the number of available LEDs should increase the probability that a carrier captures a LED segment in a given time segment. An increased capture probability would result in the reduction of the overall assembly time which we observed in our experiment. Another parameter that influenced the assembly speed was the level of agitation. The assembly speed reached a maximum when injecting and extracting 1.3 mL at a pulsating frequency of 2 Hz. Higher agitation caused removal of assembled LED segments.

The packaged devices were separated from the excess LEDs using 500 μm mesh filter and assembled onto a printed circuit board in a surface mount device configuration by hand. We applied a voltage of 3 V to the printed circuit board to test the functionality of the LEDs and interconnects [Fig. 2(f)]. The yield of the self-assembly process was 95%, which means that 5% of the devices did not function. This experiment was reproduced six times; the yields were always larger than 95%. The defects that were observed included missing and misaligned device segments. These errors were not inherent to the assembly process itself, but were caused by imperfections in both the encapsulation units and the device segments: Encapsulation units that were only partially coated with solder, device segments with partially detached metal contacts, and fragments of device segments that assembled into the encapsulation units and that blocked further assembly. In some cases, we were able to achieve defect-free assemblies by careful visual inspection to select solder-coated encapsulation units that had no defects, and by removing fragments of components from the suspension of components using a 300 μm mesh filter.

During the course of this study, we observed a number of defects that were not caused by defective components. Defects integral to self-assembly processes are most commonly related to local energy minima in the space of possible combinations or to an insufficient overall energy minimum to form a stable assembly under agitation. We were able to remove energy minima-related defects completely by introducing and optimizing the complementary shapes. For example, first encapsulation units had large openings and captured one device segment at each solder coated area. These designs could not sustain a high level of agitation; defects were created by component impaction removing previously assembled LEDs. We removed these defects completely by reducing the size of the opening, and by increasing the solder-coated areas to cover 35% of the bottom face.

The agitation was a key parameter that controlled the mixing and assembly speed. We tested two types of agitation: External acceleration by manual shaking and agitation using a pulsating liquid flow. Hand agitation under a stereomicroscope is suitable to observe the assembly process. However, it was not strong enough to agitate the components sufficiently. The translational force $F_a = ax^3\rho$ that can be exerted onto the components by external acceleration a scales with the volume x^3 of the component and the density difference ρ between the component and the solvent, whereas the drag force that opposes the movement scales linearly with the component size. As a result, it becomes increasingly difficult to agitate components with decreasing size due to the different scaling laws—components tend to accumulate in the bottom of the assembly container. Hand agitation was less reproducible as well. Our experimental results suggest that the use of a pulsating flow may be a more suitable form of agitation. The pulsating flow makes use of the drag force in a liquid flow to agitate the components. The drag force dominates the gravitational force and provides excellent mixing of the components and control over the intensity of agitation. Moreover, the disordering energy due to the drag in a liquid flow and the ordering energy due to surface tension between components can be adjusted to have similar magnitudes. This may be beneficial in self-assemblies where the level of agitation needs to be adjusted to overcome local energy minima in the space of possible combinations. The energy gain due to the surface-tension S scales with the area x^2 of the involved interfaces and is given as $E_s = Sx^2$.[12] The disordering energy due to the pulsating flow shows a similar x^2 relationship if we consider spherical components with a diameter x and a pulsating laminar flow of velocity v. The energy change as a function of the displacement x can then be calculated by integrating Stokes law and becomes $E_d = 3\pi\eta vx^2$ where η is the dynamic viscosity of the liquid. This first-order estimate illustrates that the ordering energy E_s due to the surface tension and the disordering energy E_d due to the drag in a liquid flow follow the same scaling law. We believe that the ability to adjust the disordering energy by increasing the frequency of the pulsating flow, together with the similar scaling laws, will be particularly useful in the assembly of microsystems that contain components with different dimensions and that have a density that is larger than the density of the assembly solution. Pyrex and GaN have a density that is more than two times larger than water.

We have demonstrated the self-assembly and packaging of semiconductor devices by combining geometrical shape recognition with site specific wetting and binding involving liquid solder. The LED devices that have been packaged are relatively simple devices with a small number of interconnects. Many integrated circuits require the registration and formation of large number of interconnects. We believe that shape-and-solder directed self-assembly will be useful to realize not only such systems but also multicomponent three-dimensional microsystems. The combination of shape-and-solder-directed self-assembly with hierarchical self-assembly[13] and electrically programmable self-assembly[14,15] will provide additional flexibility in the realization of such systems.

[1]C. D. Fung, P. W. Cheung, W. H. Ko, and D. G. Fleming, *Micromachining and Micropackaging of Transducers* (Elsevier, Amsterdam, 1985).

[2]J. W. Sliwa Jr., US Patent No. 5,075,253 (1991).

[3]H. J. J. Yeh and J. S. Smith, IEEE Photonics Technol. Lett. **6**, 706 (1994).

[4]J. S. Smith and H. J. J. Yeh, US Patent No. 5,824,186 (1998).

[5]D. H. Gracias, J. Tien, T. L. Breen, C. Hsu, and G. M. Whitesides, Science **289**, 1170 (2000).

[6]M. Boncheva, D. H. Gracias, H. O. Jacobs, and G. M. Whitesides, Proc. Natl. Acad. Sci. U.S.A. **99**, 4937 (2002).

[7]U. Srinivasan, D. Liepmann, and R. T. Howe, J. Microelectromech. Syst. **10**, 17 (2001).

[8]U. Srinivasan, M. A. Helmbrecht, C. Rembe, R. S. Muller, and R. T. Howe, IEEE J. Sel. Top. Quantum Electron. **8**, 4 (2002).

[9]K. F. Bohringer, U. Srinivasan, and R. T. Howe, Technical Digest. MEMS, 369 (2001).

[10]H. O. Jacobs, A. R. Tao, A. Schwartz, D. H. Gracias, and G. M. Whitesides, Science **296**, 323 (2002).

[11]T. L. Breen, J. Tien, S. R. J. Oliver, T. Hadzic, and G. M. Whitesides, Science **284**, 948 (1999).

[12]K. S. Birdi, *Self-assembly Monolayer Structures of Lipids and Macromolecules at Interfaces* (Kluwer Plenum, New York, 1999).

[13]W. A. Lopes, Nature (London) **414**, 735 (2001).

[14]X. Xiong, Y. Hanein, J. Fang, Y. Wang, W. Wang, D. T. Schwartz, and K. F. Bohringer, J. Microelectromech. Syst. **12**, 117 (2003).

[15]C. R. Barry, C. J. Hoon, and H. O. Jacobs, *Approaching Programmable Self-assembly Form Nanoparticle-based Devices to Integrated Circuits*, Snowbird, UT, 2004 (DARPA), pp. 300–308.